Available online at www.sciencedirect.com
SCIENCE DIRECT®
Journal of Organometallic Chemistry 690 (2005) 3908–3917
Journal of Organometallic Chemistry
www.elsevier.com/locate/jorganchem

Iridium mediated methyl and phenyl C–H activation of 2-(arylazo)phenols. Synthesis, structure, and spectral and electrochemical properties of some organoiridium complexes

Rama Acharyya [a], Falguni Basuli [a], Shie-Ming Peng [b], Gene-Hsiang Lee [b], Ren-Zhang Wang [c], Thomas C.W. Mak [c], Samaresh Bhattacharya [a,*]

[a] *Department of Chemistry, Inorganic Chemistry Section, Jadavpur University, Kolkata 700 032, India*
[b] *Department of Chemistry, National Taiwan University, Taipei, Taiwan, ROC*
[c] *Department of Chemistry, The Chinese University of Hong Kong, Shatin, New Territories, Hong Kong*

Received 8 March 2005; received in revised form 20 May 2005; accepted 20 May 2005
Available online 27 June 2005

Abstract

Reaction of 2-(2′,6′-dimethylphenylazo)-4-methylphenol with $[Ir(PPh_3)_3Cl]$ in refluxing ethanol in the presence of a base (NEt_3) affords an organoiridium complex **5**, where the 2-(2′,6′-dimethylphenylazo)-4-methylphenol is coordinated to iridium, via C–H activation of a methyl group, as a dianionic tridentate C,N,O-donor. Two triphenylphosphines and a hydride are also coordinated to the metal center. A similar reaction carried out in toluene affords complex **5** along with a similar complex **7**, where a chloride is coordinated to iridium instead of the hydride. Reaction of 2-(2′-methylphenylazo)-4-methylphenol with $[Ir(PPh_3)_3Cl]$ in refluxing ethanol in the presence of a base (NEt_3) affords an organoiridium complex **12**, where the 2-(2′-methylphenylazo)-4-methylphenol is coordinated to iridium, via C–H activation at the ortho position of the phenyl group in the 2′-methylphenylazo fragment, as a dianionic tridentate C,N,O-donor. Two triphenylphosphines and a hydride are also coordinated to the metal center. A similar reaction carried out in toluene affords a complex **12** along with a similar complex **13**, where a chloride is coordinated to iridium instead of the hydride. Structures of complexes **5**, **12** and **13** have been determined by X-ray crystallography. In all these complexes, the two triphenylphosphines are *trans*. All these complexes show intense MLCT transitions in the visible region. Cyclic voltammetry on all the complexes shows an Ir(III)–Ir(IV) oxidation within 0.60–0.73 V vs. SCE, followed by an oxidation of the coordinated 2-(arylazo)phenolate ligand within 1.08–1.39 V vs. SCE. A reduction of the coordinated 2-(arylazo)phenolate ligand is observed within −1.10 to −1.26 V vs. SCE.

Keywords: C–H activation; 2-(Arylazo)phenols; Organoiridium complexes; Structure; Spectral and electrochemical properties

1. Introduction

The present work has originated from a recent study in our laboratory, where we have observed that the 2-(arylazo)phenols (**1**) undergo both phenolic O–H and phenyl C–H activation upon their reaction with $[Ir(PPh_3)_3Cl]$, and afford organoiridium complexes where the 2-(arylazo)phenols are coordinated to iridium as tridentate C, N, O-donors **2** [1]. We have witnessed ligand **1** to display the same mode of coordination in several other reactions [2]. With an intention of inducing a different mode of coordination in such ligands, we have selected two modified 2-(arylazo)phenols for the present study, viz. 2-(2′,6′-dimethylphenylazo)-4-methylphenol (**3**) where both the ortho positions of the phenyl ring in arylazo fragment are blocked by methyl groups, and

* Corresponding author. Tel.: +91 332 414 6223; fax: +91 332 414 6584.
E-mail address: samaresh_b@hotmail.com (S. Bhattacharya).

0022-328X/$ - see front matter © 2005 Elsevier B.V. All rights reserved.
doi:10.1016/j.jorganchem.2005.05.025

2-(2′-methylphenylazo)-4-methylphenol (**4**) where only one ortho position is blocked by a methyl group. To study the consequences of these ligand modifications, reaction of ligands **3** and **4** has been carried out with $[Ir(PPh_3)_3Cl]$. It may be noted here that unlike its rhodium analogue, viz. the Wilkinson's catalyst $[Rh(PPh_3)_3Cl]$, reactivity of this iridium complex has been much less explored [1,3]. However, we have found it to be an excellent starting material for the synthesis of different mixed-ligand complexes of iridium [1,4]. Reaction of ligands **3** and **4** with $[Ir(PPh_3)_3Cl]$ has been found to afford interesting organoiridium complexes via C–H activation. It is relevant to mention here that metal mediated C–H activation of organic molecules has been of considerable current interest, as chemical transformations of organic molecules often proceed via a C–H activation step leading to the formation of organometallic complexes as reactive intermediates, which then undergo further reactions to yield the desired product [5]. An account of the chemistry of all the organoiridium complexes, synthesized in this study, is presented here with special reference to their formation, structure, and spectral and electrochemical properties.

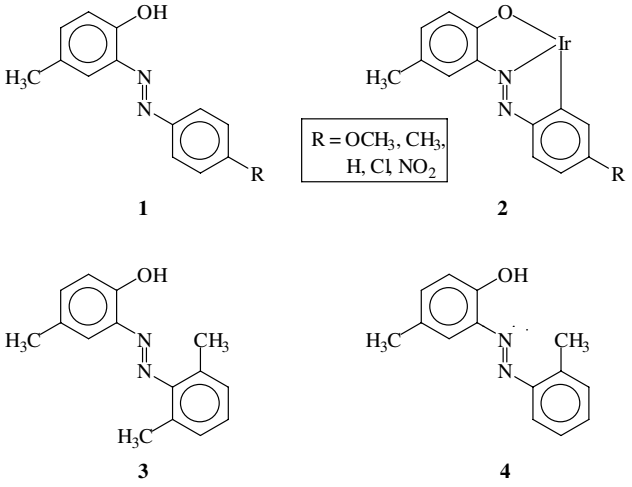

2. Results and discussion

2.1. Synthesis and characterization

Reaction of ligand **3** with $[Ir(PPh_3)_3Cl]$ proceeds smoothly in refluxing ethanol in the presence of triethylamine to afford a pink complex **5** in descent yield. Though ligand **3** contains three methyl groups, ^{1}H NMR spectrum of complex **5** shows only two methyl signals of equal intensity at 1.95 and 2.29 ppm. However, a distinct signal corresponding to two hydrogens is observed at 3.59 ppm, which is indicative of a significantly deshielded CH_2 fragment. Appearance of these three signals indicates that ligand **3** is probably coordinated to iridium as a tridentate C, N, O-donor **6** via dissociation of the phenolic proton and another proton from one methyl group in the 2′,6′-dimethylphenylazo fragment. All the six aromatic proton signals, expected from the coordinated ligand in **6**, are also clearly observed in the expected region. The ^{1}H NMR spectrum also shows a distinct triplet at −15.32 ppm indicating the presence of a coordinating hydride and broad signals within 7.17–7.43 ppm, corresponding to 30 hydrogens, attributable to two triphenylphosphines. The triplet nature of the hydride signal indicates that the two triphenylphosphines are magnetically equivalent in complex **5**. The ^{1}H NMR spectral data thus point to a definite composition and stereochemistry for complex **5**, in which a doubly deprotonated ligand **3**, two triphenylphosphines and a hydride are coordinated to the metal center and the two triphenylphosphines are mutually

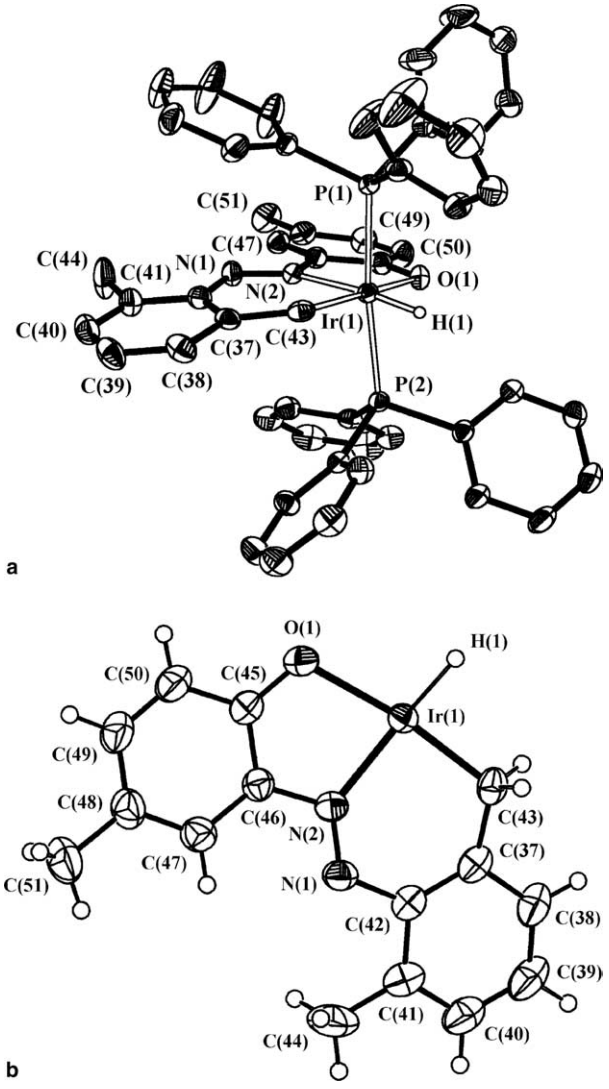

Fig. 1. View of (a) the complex **5** and (b) the equatorial plane in complex **5**.

Table 1
Selected bond lengths (Å) and bond angles (°) for complexes **5**, **12** and **13**

Complex ***5***	
Bond lengths	
Ir(1)–H(1)	1.45(3)
Ir(1)–C(43)	2.088(3)
Ir(1)–N(2)	2.074(3)
Ir(1)–O(1)	2.156(2)
Ir(1)–P(1)	2.3300(9)
Ir(1)–P(2)	2.3277(8)
C(37)–C(42)	1.410(5)
C(37)–C(43)	1.510(5)
C(45)–C(46)	1.426(5)
C(46)–N(2)	1.425(4)
C(42)–N(1)	1.427(4)
N(1)–N(2)	1.276(4)
C(45)–O(1)	1.313(4)
Bond angles	
H(1)–Ir(1)–N(2)	176.6(16)
C(43)–Ir(1)–O(1)	171.56(11)
P(1)–Ir(1)–P(2)	170.12(3)
C(43)–Ir(1)–N(2)	91.97(12)
N(2)–Ir(1)–O(1)	80.10(10)
Complex ***12***	
Bond lengths	
Ir–H(1A)	1.47(3)
Ir–N(1)	2.017(3)
Ir–O(1)	2.179(2)
Ir–P(1)	2.3059(8)
Ir–P(2)	2.3107(8)
C(7)–N(1)	1.410(4)
C(6)–N(2)	1.397(4)
N(1)–N(2)	1.276(4)
C(12)–O(1)	1.311(4)
Bond angles	
H(1A)–Ir–N(1)	174.7(11)
C(1)–Ir–O(1)	156.83(12)
P(1)–Ir–P(2)	163.05(3)
C(1)–Ir–N(1)	77.60(12)
N(1)–Ir–O(1)	79.32(9)
Complex ***13***	
Bond lengths	
Ir(1)–C(8)	2.030 (10)
Ir(1)–N(1)	1.941(8)
Ir(1)–O(1)	2.191(9)
Ir(1)–P(1)	2.349(4)
Ir(1)–P(2)	2.365(4)
Ir(1)–Cl(1)	2.395(3)
C(6)–N(1)	1.345(14)
C(7)–N(2)	1.438(14)
N(1)–N(2)	1.312(12)
C(1)–O(1)	1.312(13)
Bond angles	
C(8)–Ir(1)–O(1)	158.4(4)
N(1)–Ir(1)–Cl(1)	173.3(3)
P(1)–Ir(1)–P(2)	172.42(11)
C(8)–Ir(1)–N(1)	77.9(4)
N(1)–Ir(1)–O(1)	80.5(4)

trans. The observed microanalytical data of complex **5** are also consistent with this composition. To verify the stereochemistry of complex **5**, as well as the coordination mode of ligand **3** in it, its structure has been determined by X-ray crystallography. The structure is shown in Fig. 1 and relevant bond parameters are listed in Table 1. The structure shows that all the indications given by the ^{1}H NMR spectrum are indeed correct. Ligand **3** is coordinated to iridium as a C, N, O-donor **6**, with bite angles of 80.10(10)° [O(1)–Ir(1)–N(2)] and 91.97(12)° [C(43)–Ir(1)–N(2)]. Two triphenylphosphines and a hydride are also coordinated to the metal center. Iridium is thus sitting in a $HCNOP_2$ coordination sphere, which is significantly distorted from ideal octahedral geometry as reflected in the bond parameters around the metal center. The coordinated ligand **3** and the hydride are sharing the same equatorial plane with iridium at the center, and the two triphenylphosphines have occupied the remaining two axial positions. The Ir–H and Ir–P distances are quite normal and so are the Ir–C, Ir–N, Ir–O, C–O and N–N bond lengths within the C, N, O-chelated fragment **6** [1,6]. The observed C–H activation of a methyl group in ligand **3** has been quite interesting, and it may be mentioned here that though ligand **3** has recently been observed to undergo interesting chemical transformations via migration of one methyl group [7], such a methyl C–H activation of ligand **3** has been observed for the first time. It is also worth noting here that compared to phenyl C–H activation, methyl C–H activation is relatively less common [8].

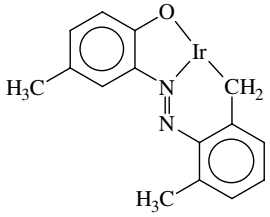

6

The presence of a hydride in complex **5** has also been quite interesting. Two sources of the hydride seem probable, ethanol may serve as a source of the hydride, or oxidative insertion of iridium(I) into the phenolic O–H bond may generate a hydride. To check this, reaction of ligand **3** with $[Ir(PPh_3)_3Cl]$ has also been carried out in a nonalcoholic solvent, viz. toluene, in the presence of triethylamine. A mixture of two complexes, with distinctly different colors (pink and purple), has been obtained from this reaction. The individual complexes have been separated by chromatography. The combined yield of the two complexes has been satisfactory. Characterization on the pink complex has confirmed it to be the same complex **5**, which was obtained as the sole product from the ethanol reaction. However, the purple complex has been found to be different. ^{1}H NMR spectrum of the purple complex does not show any hydride

signal. Besides that, rest of the ^{1}H NMR spectrum of the purple complex is qualitatively similar to that of complex **5**. Infrared spectrum of this purple complex indicates the presence of a coordinated chloride in it (vide infra). The ^{1}H NMR and IR spectral data thus show that the purple complex has a similar composition as complex **5**, except that a chloride is coordinated to iridium instead of a hydride, and hence we assume a structure **7** for this purple complex (henceforth referred to as complex **7**). Structural characterization of complex **7** by X-ray crystallography has not been possible, as its crystals could not be grown. However, *trans* disposition of two triphenylphosphines has been confirmed by the ^{31}P NMR spectrum of this complex, which shows a single resonance at 50.20 ppm.

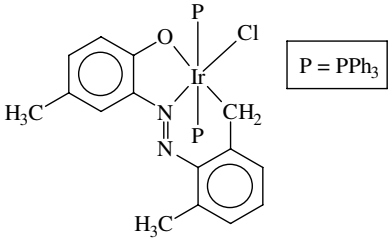

7

Formation of the hydride complex **5** in addition to its chloride analogue **7** from the reaction carried out in toluene clearly shows that ethanol has not been the source of hydride in complex **5** in the earlier synthetic reaction. The exact mechanism of the synthetic reactions is not completely clear to us. However, the sequences shown in Scheme 1 seem probable. In the initial step, ligand **3** binds to the metal center in $[Ir(PPh_3)_3Cl]$ via oxidative insertion of iridium into the phenolic O–H bond, and simultaneous dissociation of one triphenylphosphine, and thus affords two geometric isomers of a reactive intermediate (complexes **8** and **9**). These intermediates then undergo cyclometalation via elimination of either HCl (in case of **8**) or H_2 (in case of **9**) affording complexes **5** and **7**, respectively. It seems that in the ethanol reaction only the intermediate **8** is formed, and its isomerization to complex **9** could not take place because of the relatively low boiling point of ethanol. Isolation of these speculated intermediates has not been possible probably due to their rapid transformation into the corresponding cyclometalated species.

Facile C–H activation of the methyl group in ligand **3**, observed on its reaction with $[Ir(PPh_3)_3Cl]$, encouraged us to explore the possibility of such C–H activation in similar ligands. Thus, we have selected 2-(2′-methylphenylazo)-4-methylphenol (**4**) as the next ligand. This particular ligand has been chosen because in it only one *ortho* position of the phenyl ring in the arylazo fragment is blocked by a methyl group, while the other ortho

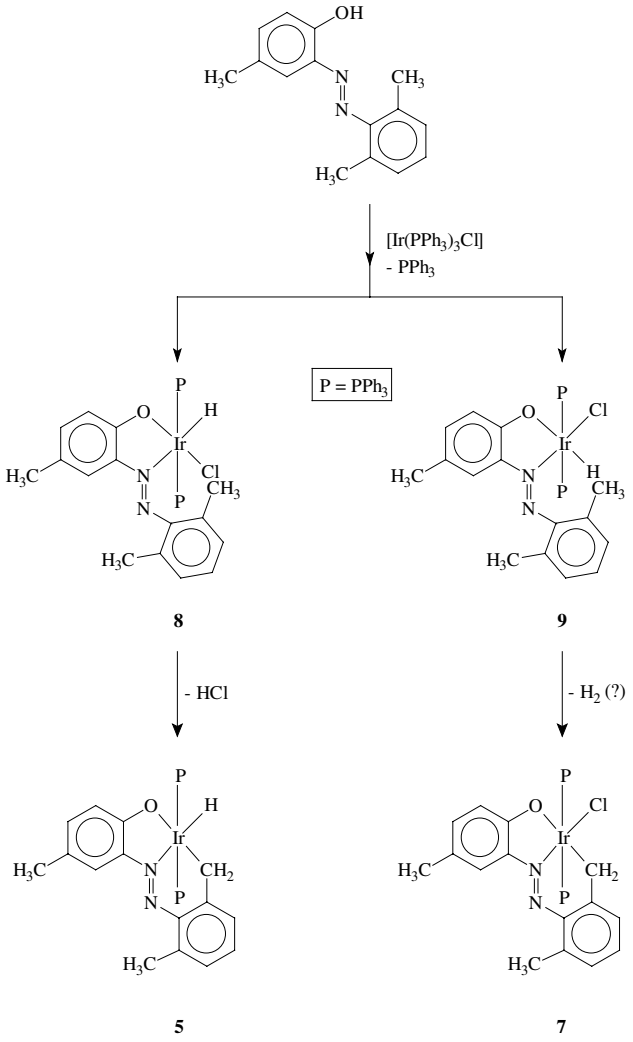

Scheme 1. Probable steps of the synthetic reactions.

position is still unsubstituted. Hence, two types of C–H activation, viz. methyl C–H activation and phenyl C–H activation, are in principle possible in this ligand affording cyclometallated species of type **10** and **11**, respectively. To check the preference of C–H activation, if any, of ligand **4**, its reaction with $[Ir(PPh_3)_3Cl]$ has been carried out in refluxing ethanol in the presence of triethylamine, which has afforded a blue complex **12**. ^{1}H NMR spectrum of this complex shows two methyl signals at 1.94 and 2.31 ppm and thus excludes the possibility of linkage isomer **10**. Structure of this complex **12** has been determined by X-ray crystallography. The structure (Fig. 2) shows that ligand **4** is coordinated as shown in **11**. Two triphenylphosphines and a hydride are also coordinated to the metal center. The observed bond distances (Table 1) compare well with those in complex **5**. To investigate whether a chloride analogue of complex **12** can be obtained from a non-alcoholic solvent, reaction of ligand **4** with $[Ir(PPh_3)_3Cl]$ has also been carried out in refluxing toluene in the presence of

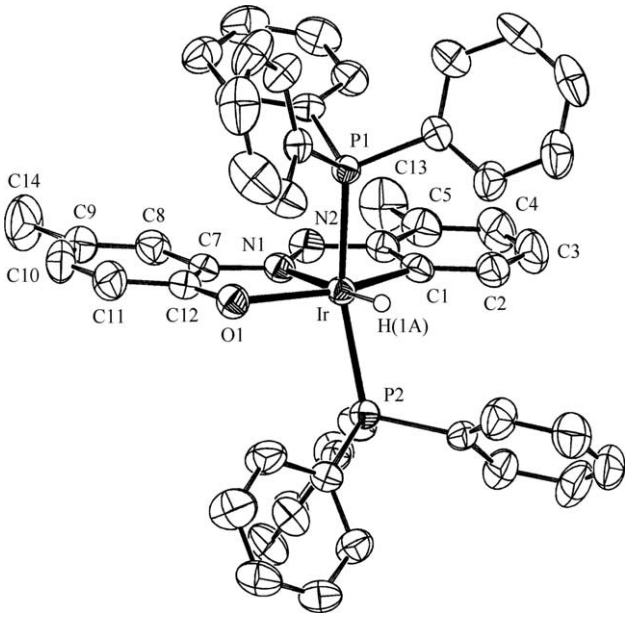

Fig. 2. View of the complex **12**.

triethylamine. A mixture of two blue complexes has been obtained from this reaction, which have been separated by chromatography. The blue complex, which moves faster through the column, has been found to be complex **12**. The other blue complex, which moves relatively slowly through the column, has been found to be the chloride analogue of complex **12**. This second blue complex, henceforth referred to as complex **13**, has also been structurally characterized. The structure (Fig. 3) shows that complex **13** has a similar structure as complex **12**, except that the position of hydride in **12** is occupied by a chloride in **13**. The Ir–Cl bond length is normal [1] and the other bond parameters around iridium in complex **13** are found to be similar to those observed in complex **12**. Besides the absence of the hydride signal, ^{1}H NMR spectrum of complex **13** is very similar to that of complex **12**. The difference in the number and nature of the product in two different solvents viz. ethanol and toluene may be rationalized as explained in Scheme 1.

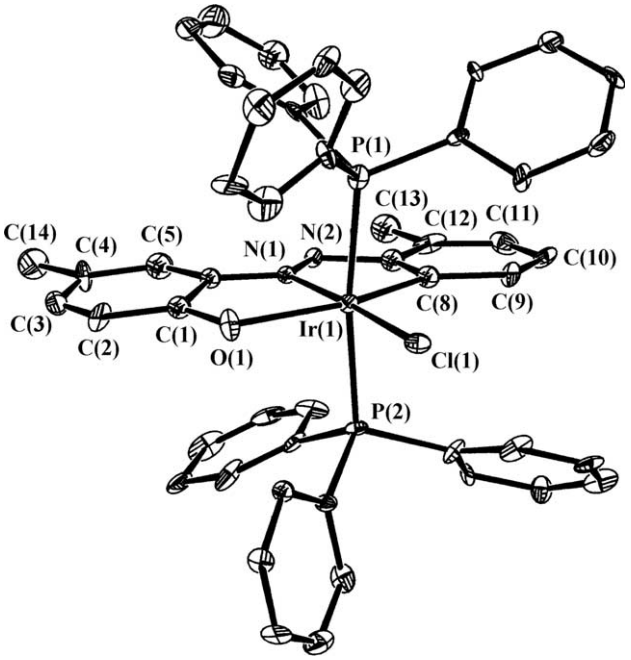

Fig. 3. View of the complex **13**.

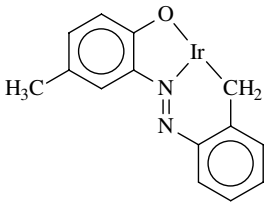

10

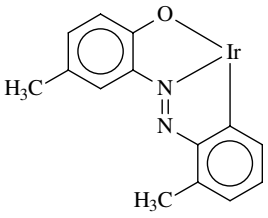

11

2.2. Spectral studies

Infrared spectra of all the complexes show many sharp and strong bands of different intensities within 2200–200 cm^{-1}. Attempt has not been made to assign each individual band to a specific vibration. However, the presence of three strong bands near 515, 695 and 750 cm^{-1} in all the complexes is attributable to the coordinated PPh_3 ligands. In complexes **5** and **12**, a sharp band is observed at 2110 and 2050 cm^{-1}, respectively, which is assigned to the Ir–H stretch. In complexes **7** and **13**, the Ir–Cl stretch has been observed at 295 and 293 cm^{-1}, respectively. Electronic spectra of the complexes have been recorded in dichloromethane solution. Each complex shows several intense absorptions in the visible and ultraviolet region (Table 2). The absorptions in the ultraviolet region are believed to be due to transitions within the ligand orbitals, and those in the visible region are probably due to metal-to-ligand charge-transfer transitions. To have an insight into the nature of absorptions in the visible region, qualitative EHMO calculations have been performed [9] on computer-generated models of all the four complexes, where phenyl rings of the triphenylphosphines have been replaced by hydrogens. The results are found to be qualitatively similar for all the complexes [10]. Compositions of selected molecular orbitals are given in Table 3 and partial MO diagram of a selected complex is shown in Fig. 4. Partial MO diagrams of the other three complexes are deposited as supporting information (Fig. S1–S3). The highest occupied molecular orbital (HOMO) and the next two filled orbitals (HOMO − 1 and HOMO − 2) have major contribution from the iridium d_{xy}, d_{yz} and d_{zx} orbitals

Table 2
Electronic spectral and cyclic voltammetric data

Compound	Electronic spectral data λ_{max}, nm (ε, M^{-1} cm^{-1})[a]	Cyclic voltammetric data[b] E, V vs. SCE
Complex **5**	548(13,600), 406(7200)[c], 346(17,200), 292(26,400)[c], 266(44300)[c]	1.15[d], 0.64[d], −1.22[e]
Complex **7**	606(13,100), 572(12,850), 406(14,600)[c], 340(25,800), 268(51,300)	1.08[d], 0.60[d], −1.26[e]
Complex **12**	604(6400), 574(6000)[c], 412(4000)[c], 342(10,100), 278(22,000)[c]	1.22[d], 0.64(67)[f], −1.23[e]
Complex **13**	644(3100), 600(2800), 388(3700), 354(5600)[c], 338(5700), 258(20,700)	1.39[d], 0.73(60)[f], −1.10[e]

[a] In dichloromethane.
[b] Solvent, 1:9 dichloromethane-acetonitrile; supporting electrolyte, TBAP; scan rate 50 mVs^{-1}.
[c] Shoulder.
[d] E_{pa} value.
[e] E_{pc} value.
[f] $E_{1/2}$ value (ΔE_p value), where $E_{1/2} = 0.5\ (E_{pa} + E_{pc})$ and $\Delta E_p = (E_{pa} - E_{pc})$.

Table 3
Composition of selected molecular orbitals

Compound	Contributing fragments	% Contribution of fragments to					
		HOMO	HOMO − 1	HOMO − 2	LUMO	LUMO + 1	LUMO + 2
Complex **5**	Ir	63	65	20	14	–	–
	Ligand	33	27	75	86	97	95
	azo	6	–	–	54	–	–
Complex **7**	Ir	71	65	64	15	–	–
	Ligand	24	27	33	79	97	95
	azo	–	–	–	52	–	–
Complex **12**	Ir	84	58	66	12	–	–
	Ligand	7	36	25	83	94	96
	azo	–	–	–	53	–	–
Complex **13**	Ir	84	61	64	17	–	48
	Ligand	5	34	29	80	97	43
	azo	–	–	–	47	–	–

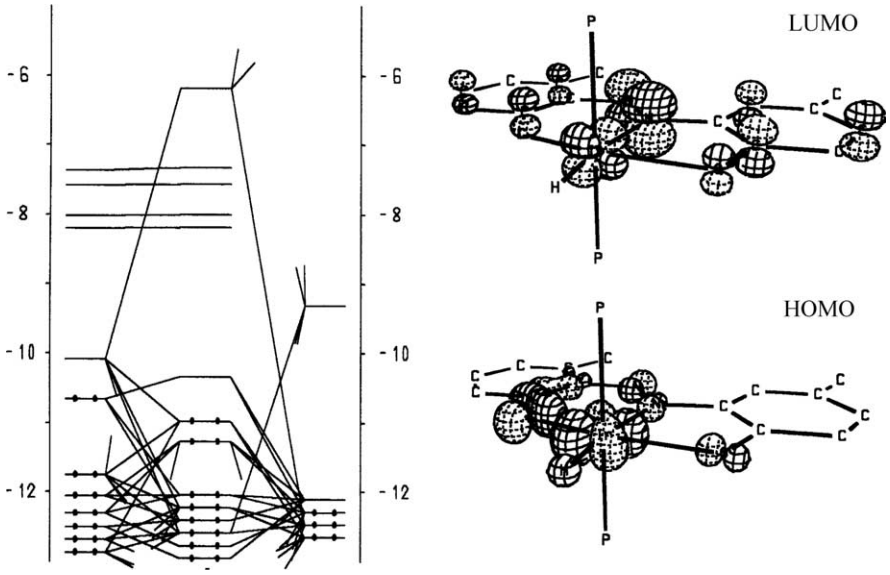

Fig. 4. Partial molecular orbital diagram of complex **5**.

[10]. These three filled orbitals may therefore be regarded as iridium-t_2 orbitals. The lowest unoccupied molecular orbital (LUMO) has $\geqslant$80% contribution from the 2-(arylazo)phenolate ligands and is concentrated mostly ($\geqslant$50%) on the azo fragment. The LUMO + 1 and LUMO + 2 are localized on other parts

of the 2-(arylazo)phenolate ligands. The lowest energy absorption in the visible region is therefore assignable to an allowed charge-transfer transition from the filled iridium-t_2 orbital (HOMO) to the vacant π* (azo)-orbital of the 2-(arylazo)phenolate ligand (LUMO). The other intense absorptions in the visible region may be assigned to charge-transfer transitions from the filled t_2 orbitals to the higher energy vacant orbitals.

2.3. Electrochemical properties

Electrochemical properties of all the complexes have been studied by cyclic voltammetry in 1:9 dichloromethane–acetonitrile solution (0.1 M TBAP) [11]. Voltammetric data are given in Table 2. Each complex shows two oxidative responses on the positive side of SCE and a reductive response on the negative side. In view of the results of the EHMO calculations, the first oxidative response is assigned to Ir(III)–Ir(IV) oxidation and the reductive response is assigned to reduction of the azo function of the coordinated 2-(arylazo)phenolate ligand. The second oxidative response is tentatively assigned to oxidation of the coordinated 2-(arylazo)phenolate ligand. In complex **5**, the Ir(III)–Ir(IV) oxidation has been found to be completely irreversible, however, in complex **7** the same is found to be quasi-reversible. In complexes **12** and **13** the Ir(III)–Ir(IV) oxidation has been found to be reversible, characterized by a peak-to-peak separation (E_p) of about 60 mV, which remains unchanged upon variation of scan rate, and the anodic peak-current (i_{pa}) is also found to be equal to the cathodic peak-current (i_{pc}), as expected for a reversible couple. The ligand oxidation, as well as the ligand reduction, have been found to be irreversible in all the complexes. One-electron nature of the Ir(III)–Ir(IV) oxidation has been established by comparing its current height (i_{pa}) with that of standard ferrocene–ferrocenium couple under identical experimental conditions. The irreversible redox responses have been found to show non-stoichiometric currents.

3. Conclusions

The present study shows that C–H activation of suitable alkyl groups, introduced into the *ortho* positions of the phenyl ring in the arylazo fragment of 2-(arylazo)phenols (**1**) can be easily achieved by reacting such ligands with $[Ir(PPh_3)_3Cl]$. Such studies involving ligands of type **14** are currently in progress. The present study also shows that in ligands of type **15**, where two types of C–H activation is possible, the C–H activation at the unsubstituted ortho position of the aryl ring is much more likely compared to C–H activation of the alkyl ($-CHR_1R_2$) group.

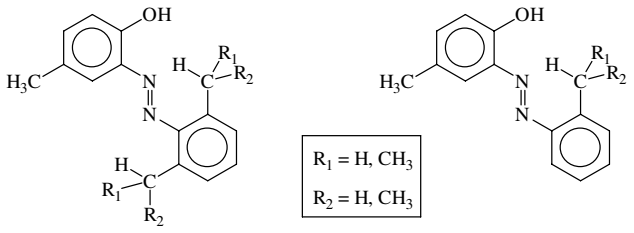

14 **15**

4. Experimental

Iridium trichloride was purchased from Arora Matthey, Kolkata, India, and 2,6-dimethylaniline was obtained from Loba, Mumbai, India. 2-Methylaniline and *p*-cresol were purchased from S.D., India. The 2-(arylazo)phenols were prepared by coupling respective diazotized aniline with *p*-cresol. $[Ir(PPh_3)_3Cl]$ was prepared as before [1]. Purification of acetonitrile and dichloromethane, and preparation of tetrabutylammonium perchlorate (TBAP) for electrochemical work were performed as reported in the literature [12]. Microanalyses (C, H, N) were performed using a Perkin–Elmer 240C elemental analyzer. IR spectra were obtained on a Perkin–Elmer 1601 spectrometer with samples prepared as KBr pellets. Electronic spectra were recorded on a JASCO V-570 spectrophotometer. NMR spectra were recorded in $CDCl_3$ solution using a Bruker drx500 or Bruker Avance dpx300 NMR spectrometer. Electrochemical measurements were made using a CH Instruments model 600A electrochemical analyzer. A platinum disc working electrode, a platinum wire auxiliary electrode and an aqueous saturated calomel reference electrode (SCE) were used in the cyclic voltammetry experiments. All electrochemical experiments were performed under a dinitrogen atmosphere. All electrochemical data were collected at 298 K and are uncorrected for junction potentials.

4.1. Synthesis of complexes

4.1.1. Complex 5

2-(2′,6′-Dimethylphenylazo)-4-methylphenol (25 mg, 0.10 mmol) was dissolved in ethanol (50 mL) and the solution was purged with a stream of dinitrogen for 5 min. To the solution were added triethylamine (20 mg, 0.20 mmol) and $[Ir(PPh_3)_3Cl]$ (100 mg, 0.10 mmol) successively. The mixture was refluxed under a dinitrogen atmosphere for 24 h, when a red solution was obtained. Evaporation of this solution afforded a red solid, which was purified by thin layer chromatography on a silica plate with benzene as the eluant. A pink band separated, which was extracted with acetonitrile. Upon slow

evaporation of the acetonitrile extract complex **5** was obtained as a crystalline pink solid. Yield: 60%.

Anal. Calc. for $C_{51}H_{45}N_2OP_2Ir$ (**5**): C, 64.08; H, 4.71; N, 2.93. Found: C, 64.00; H, 4.67; N, 2.95%. ^{1}H NMR [13]: −15.32 (t, hydride, $J = 18.6$), 1.95 (CH_3), 2.29 (CH_3), 3.59 (t, CH_2, $J = 10.2$), 6.14 (d, 1H, $J = 7.4$), 6.36 (d, 1H, $J = 8.5$), 6.50–6.64 (2H*), 6.67 (s, 1H), 6.85 (d, 1H, $J = 7.1$), 7.17–7.43 ($2PPh_3$).

4.1.2. Complex 7

This complex was prepared by following the same above procedure using toluene instead of ethanol and the refluxing time was 48 h. Purification was achieved by thin layer chromatography on a silica plate with benzene as the eluant. Two bands (pink and purple) separated, which were extracted with acetonitrile. Upon slow evaporation of the pink and purple extracts complex **5** (Yield: 35%) and **7** (Yield: 20%) were obtained, respectively, as crystalline solids.

Anal. Calc. for $C_{51}H_{44}N_2OP_2ClIr$ (**7**): C, 61.85; H, 4.45; N, 2.83. Found: C, 61.53; H, 4.37; N, 2.89%. ^{1}H NMR [13]: 1.82 (CH_3), 2.29 (CH_3), 5.01 (t, CH_2, $J = 10.0$), 6.12 (d, 1H, $J = 7.2$), 6.50 (d, 1H, $J = 7.5$), 6.60 (s, 1H), 6.79 (t, 1H, $J = 7.3$), 7.00 (d, 1H, $J = 7.0$), 7.03–7.64 ($2PPh_3$). ^{31}P NMR: 50.20 (s).

4.1.3. Complex 12

2-(2′-Methylphenylazo)-4-methylphenol (25 mg, 0.11 mmol) was dissolved in ethanol (50 mL) and the solution was purged with a stream of dinitrogen for 5 min. To the solution were added triethylamine (20 mg, 0.20 mmol) and $[Ir(PPh_3)_3Cl]$ (100 mg, 0.10 mmol) successively. The mixture was refluxed under a dinitrogen atmosphere for 12 h, when a blue solution was obtained. Evaporation of this solution afforded a blue solid, which was purified by thin layer chromatography on a silica plate with benzene as the eluant. A blue band separated, which was extracted with acetonitrile. Slow evaporation of the eluate gave complex **12** as a crystalline solid. Yield: 70%.

Anal. Calc. for $C_{50}H_{43}N_2OP_2Ir$ (**12**): C, 63.76; H, 4.57; N, 2.98. Found: C, 64.00; H, 4.63; N, 3.01%. ^{1}H NMR [13]: −12.29 (t, hydride, $J = 18.0$), 1.94 (CH_3), 2.31 (CH_3), 5.95 (t, 1H, $J = 7.3$), 6.09 (d, 1H, $J = 7.6$), 6.25 (d, 1H, $J = 8.7$), 6.33 (d, 1H, $J = 7.2$), 6.43 (s, 1H), 6.50 (d, 1H, $J = 8.8$), 7.12–7.50 ($2PPh_3$).

4.1.4. Complex 13

This complex was prepared by following the same above procedure using toluene instead of ethanol and the refluxing time was 24 h. Purification was achieved by thin layer chromatography on a silica plate with benzene as the eluant. Two blue bands separated, which were extracted with acetonitrile. Slow evaporation of these extracts gave complex **12** (Yield: 40%) and complex **13** (Yield: 32%) as crystalline solids.

Anal. Calc. for $C_{50}H_{42}N_2OP_2ClIr$ (**13**): C, 61.51; H, 4.31; N, 2.87. Found: C, 61.77; H, 4.37; N, 2.89%. ^{1}H NMR [13]: 1.79 (CH_3), 2.37 (CH_3), 5.87 (s, 1H), 6.26 (d, 1H, $J = 8.9$), 6.32 (d, 1H, $J = 7.6$), 6.38–6.50 (2H*), 6.92 (d, 1H, $J = 7.4$), 7.02–7.59 ($2PPh_3$).

4.2. X-ray structure determination

Single crystals of complexes **5** and **12** were obtained by slow evaporation of acetonitrile solutions of the

Table 4
Selected crystallographic data for the complexes **5**, **12** and **13**

	Complex **5**	Complex **12**	Complex **13**
Empirical formula	$C_{51}H_{45}N_2OP_2Ir$	$C_{50}H_{43}N_2OP_2Ir$	$C_{50}H_{42}N_2OP_2ClIr$
F_w	956.03	942.00	976.45
Space group	Triclinic, $P\bar{1}$	Monoclinic, $P2_1/c$	Triclinic, $P\bar{1}$
Unit cell dimensions			
a (Å)	11.1750(12)	17.4737(6)	10.0981(5)
b (Å)	11.3021(12)	10.2005(4)	11.8715(6)
c (Å)	18.8872(19)	23.1955(9)	17.9205(9)
α (°)	89.168(2)	90	99.7520(10)
β (°)	87.418(2)	92.798(1)	91.8930(10)
γ (°)	61.819(2)	90	95.6850(10)
V (Å^3)	2100.5(4)	4129.4(3)	2104.13(18)
Z	2	4	2
λ (Å)	0.71073	0.71073	0.71073
Crystal size (mm)	$0.42 \times 0.30 \times 0.14$	$0.35 \times 0.35 \times 0.10$	$0.50 \times 0.30 \times 0.20$
T (K)	293(2)	295(2)	273(2)
μ (m^{-1})	3.295	3.351	3.353
R_1[a]	0.0296	0.0277	0.0301
WR_2[b]	0.0741	0.0633	0.0823
Goodness-of-fit[c]	1.012	1.076	0.705

[a] $R_1 = \Sigma\|F_o| - |F_c\|/\Sigma|F_o|$.
[b] $wR_2 = [\Sigma\{w(F_o^2 - F_c^2)^2\}/\Sigma\{w(F_o^2)\}]^{1/2}$.
[c] GOF $= [\Sigma(w(F_o^2 - F_c^2)^2)/(M - N)]^{1/2}$, where M is the number of reflections and N is the number of parameters refined.

respective complexes. Crystals of complex **13** were grown by slow diffusion of hexane into a dichloromethane solution of the complex. Selected crystal data and data collection parameters are given in Table 4. Data were collected on a Siemens Smart CCD diffractometer using graphite monochromated Mo Kα radiation ($\lambda = 0.71073$ Å) by ϕ and ω scans. X-ray data reduction, and structure solution and refinement were done using SHELXS-97 and SHELXL-97 programs [14]. The structures were solved by direct methods.

Acknowledgments

Financial assistance received from the Department of Science and Technology, New Delhi, India [Grant No. SR/S1/IC-15/2004] is gratefully acknowledged. The authors thank the RSIC at Central Drug Research Institute, Lucknow, India, for the C, H, N analysis data, and the Department of Chemistry, Indian Institute of Technology – Kanpur, India, for the X-ray diffraction data of complex **13**. Thanks also to Dr. Surajit Chattopadhyay, Department of Chemistry, Kalyani University, for his help with the IR spectral measurements. R.A. thanks the Council of Scientific and Industrial Research, New Delhi for her fellowship [Grant No. 9/96(438)2004 – EMR-I].

Appendix A. Supplementary data

Crystallographic data for structural analysis have been deposited with the Cambridge Crystallographic Data Centre, CCDCs 265561–265563 for complex **5**, **12** and **13**, respectively. Copies of this information may be obtained free of charge from The Director, CCDC, 12 Union Road, Cambridge, CB2 1EZ, UK, fax (int code): +44 1223 336 033, or email: deposit@ccdc.cam.ac.uk or www: http://www.ccdc.cam.ac.uk. Partial molecular orbital diagrams of complex **7** (Fig. S1), complex **12** (Fig. S2), and complex **13** (Fig. S3) are available as supporting information. Supplementary data associated with this article can be found, in the online version at doi:10.1016/j.jorganchem.2005.05.025.

References

[1] R. Acharyya, F. Basuli, R.Z. Wang, T.C.W. Mak, S. Bhattacharya, Inorg. Chem. 43 (2004) 704.
[2] (a) P. Gupta, R.J. Butcher, S. Bhattacharya, Inorg. Chem. 42 (2003) 5405;
(b) K. Majumder, S.M. Peng, S. Bhattacharya, J. Chem. Soc., Dalton Trans. (2001) 284;
(c) S. Dutta, S.M. Peng, S. Bhattacharya, J. Chem. Soc., Dalton Trans. (2000) 4623.
[3] (a) E.J. Kuhlmann, J.J. Alexander, J. Organomet. Chem. 174 (1979) 81;
(b) E. Mueller, C. Beissner, Chemiker-Zeitung 96 (1972) 170;
(c) M.A. Bennett, D.L. Milner, Chem. Commun. 12 (1967) 581.
[4] R. Acharyya, S. Basu, S.M. Peng, G.H. Lee, S. Bhattacharya, unpublished results.
[5] (a) R.H. Crabtree, J. Chem. Soc., Dalton Trans. (2003) 3985;
(b) C.B. Pamplin, P. Legzdins, Acc. Chem. Res. 36 (2003) 223;
(c) V. Ritleng, C. Sirlin, M. Pfeffer, Chem. Rev. 102 (2002) 1731;
(d) C. Slugovc, I. Padilla-Martnez, S. Sirol, E. Carmona, Coord. Chem Rev. 213 (2001) 129;
(e) C. Jia, T. Kitamura, Y. Fujiwara, Acc. Chem. Res. 34 (2001) 633;
(f) J. Tsuji, Transition metal reagents and catalysts, Wiley-VCH, Weinheim, 2000;
(g) M. Bellar, C. Bolm (Eds.), Transition Metals for Organic Synthesis, vols. 1–2, Wiley-VCH, Weinheim, 1998;
(h) L.S. Hegedus, Coord. Chem Rev. 168 (1998) 49;
(i) B. Cornils, W.A. Hermann (Eds.), Applied homogeneous catalysis with organometallic compounds: A comprehensive handbook in two volumes, VCH, Weinheim, 1996;
(j) L.S. Liebeskind (Ed.), Advances in metal-organic chemistry, Jai Press, Greenwich, CT, 1996;
(k) E. Abel, F.G.A. Stone, G. Wilkinson (Eds.), Comprehensive organometallic chemistry, 12, Pergamon Press, Oxford, 1995;
(l) L.S. Hegedus, Transition metals in the synthesis of complex organic molecules, Mill Valley, CA, 1994;
(m) J.P. Collman, L.S. Hegedus, J.R. Norton, R.G. Finke, Principles and applications of organotransition metal chemistry, Mill Valley, CA, 1987;
(n) B.M. Trost, T.R. Verhoeven, E. Abel, in: F.G.A Stone, G. Wilkinson (Eds.), Comprehensive organometallic chemistry, vol. 8, Pergamon Press, Oxford, 1982.
[6] (a) G. Canepa, E. Sola, M. Martin, F.J. Lahoz, L.A. Ora, H. Werner, Organometallics 22 (2003) 2151;
(b) K.K.W. Lo, C.K. Chung, D.C.M. Ng, N. Zhu, New. J. Chem. 26 (2002) 81;
(c) D.A. Ortmann, B. Weberndorfer, K. Ilg, M. Laubender, H. Werner, Organometallics 21 (2002) 2369;
(d) F. Torres, E. Sola, M. Martin, C. Ochs, G. Picazo, J.A. Lopez, F.J. Lahoz, L.A. Oro, Organometallics 20 (2001) 2716;
(e) H. Werner, A. Heohn, M. Schulz, J. Chem. Soc., Dalton Trans. (1991) 777.
[7] (a) S. Nag, P. Gupta, R.J. Butcher, S. Bhattacharya, Inorg. Chem. 43 (2004) 4814;
(b) R. Acharyya, S.M. Peng, G.H. Lee, S. Bhattacharya, Inorg. Chem. 42 (2003) 7378.
[8] (a) M. Akhter, K.A. Azam, S.M. Azad, S.E. Kabir, K.M. Abdul Malik, R. Mann, Polyhedron 22 (2003) 355;
(b) S.P. Tunik, I.A. Balova, M.E. Borovitov, E. Norlander, M. Haukka, T.A. Pakknen, J. Chem. Soc., Dalton Trans. (2002) 827;
(c) R.L. Zuckerman, S.W. Krska, R.G. Bergman, J. Organomet. Chem. 608 (2000) 172;
(d) A. Zucca, M.A. Cinellu, M.V. Pinna, S. Stoccoro, G. Minghetti, M. Manassero, M. Sansoni, Organometallics 19 (2000) 4295;
(e) J.A.M. Brandts, E. Kruiswijk, J. Boersma, A.L. Spek, G. Van Koten, J. Organomet. Chem. 585 (1999) 93;
(f) J.R. Torkelson, R. McDonald, M. Cowie, Organometallics 18 (1999) 4134;
(g) P.J. Alaimo, R.G. Bergman, Organometallics 18 (1999) 2707;
(h) H.F. Luecke, R.G. Bergman, J. Am. Chem. Soc. 119 (1997) 11538;
(i) H.F. Luecke, B.A. Arndtsen, P. Burger, R.G. Bergman, J. Am. Chem. Soc. 118 (1996) 2517.
[9] (a) C. Mealli, D.M. Proserpio, CACAO Version 4.0, Italy, 1994;
(b) C. Mealli, D.M. Proserpio, J. Chem. Educ. 67 (1990) 399.

[10] The HOMO − 2 in complex **5** has less metal character.
[11] A little dichloromethane was necessary to take the complex into solution. Addition of large excess of acetonitrile was necessary to record the redox responses in proper shape.
[12] (a) D.T. Sawyer Jr., J.L. Roberts, Experimental Electrochemistry for Chemists, Wiley, New York, 1974, pp. 167–215;
(b) M. Walter, L. Ramaley, Anal. Chem. 45 (1973) 165.
[13] Chemical shifts are given in ppm and multiplicity of the signals along with the associated coupling constants (J in Hz) are given in parentheses. Overlapping signals are marked with an asterisk.
[14] G.M. Sheldrick, SHELXS-97 and SHELXL-97, Fortran Programs for Crystal Structure Solution and Refinement, University of Gottingen, Gottingen, Germany, 1997.